Research Article

Screening of novel synthetic derivatives of dehydroepiandrosterone for antivirals against flaviviruses infections

Muhammad Imran [a,b,c,d,1], Luping Zhang [a,b,c,1], Bohan Zheng [a,b,c], Zikai Zhao [a,b,c], Dengyuan Zhou [a,b,c], Shengfeng Wan [e], Zheng Chen [f,g], Hongyu Duan [a,b,c], Qiuyan Li [a,b,c], Xueqin Liu [h], Shengbo Cao [a,b,c], Shaoyong Ke [i,**], Jing Ye [a,b,c,*]

[a] State Key Laboratory of Agricultural Microbiology, Huazhong Agricultural University, Wuhan, 430070, China
[b] Key Laboratory of Preventive Veterinary Medicine in Hubei Province, College of Veterinary Medicine, Huazhong Agricultural University, Wuhan, 430070, China
[c] The Cooperative Innovation Center for Sustainable Pig Production, Huazhong Agricultural University, Wuhan, 430070, China
[d] Department of Pathology, Faculty of Veterinary Science, University of Agriculture, Faisalabad, 38040, Pakistan
[e] Department of Nephrology, Henan Provincial Key Laboratory of Kidney Diseases and Immunology, Henan Provincial People's Hospital, Zhengzhou, 450003, China
[f] Key Laboratory for Animal Health of Jiangxi Province, Nanchang, 330045, China
[g] Department of Preventive Veterinary Medicine, College of Animal Science and Technology, Jiangxi Agricultural University, Nanchang, 330045, China
[h] College of Fisheries, Huazhong Agricultural University, Wuhan, 430070, China
[i] National Biopesticide Engineering Research Center, Hubei Biopesticide Engineering Research Center, Hubei Academy of Agricultural Sciences, Wuhan, 430070, China

ARTICLE INFO

ABSTRACT

Flaviviruses are important arthropod-borne pathogens that represent an immense global health problem. Their unprecedented epidemic rate and unpredictable clinical features underscore an urgent need for antiviral interventions. Dehydroepiandrosterone (DHEA) is a natural occurring adrenal-derived steroid in the human body that has been associated in protection against various infections. In the present study, the plaque assay based primary screening was conducted on 32 synthetic derivatives of DHEA against Japanese encephalitis virus (JEV) to identify potent anti-flaviviral compounds. Based on primary screening, HAAS-AV3026 and HAAS-AV3027 were selected as hits from DHEA derivatives that exhibited strong antiviral activity against JEV (IC$_{50}$ = 2.13 and 1.98 μmol/L, respectively) and Zika virus (ZIKV) (IC$_{50}$ = 3.73 and 3.42 μmol/L, respectively). Mechanism study indicates that HAAS-AV3026 and HAAS-AV3027 do not exhibit inhibitory effect on flavivirus binding and entry process, while significantly inhibit flavivirus infection at the replication stage. Moreover, indirect immunofluorescence assay, Western blot analyses, and quantitative reverse transcription-PCR (qRT-PCR) revealed a potent antiviral activity of DHEA derivatives hits against JEV and ZIKV in terms of inhibition of viral infection, protein production, and viral RNA synthesis in Vero cells. Taken together, our results may provide a basis for the development of new antivirals against flaviviruses.

1. Introduction

Arboviruses are a significant public health concern worldwide, and are the most important medical human pathogens belong to the family *Flaviviridae*. Japanese encephalitis virus (JEV), West Nile virus (WNV), Zika virus (ZIKV), yellow fever virus (YFV), and dengue virus (DENV) are important members of the family *Flaviviridae*, genus *Flavivirus* (Imran et al., 2019; Mackenzie et al., 2004). Among these viruses, JEV is the main cause of childhood viral encephalitis in the Asia Pacific region with around 68,000 cases and 10,000 to 15,000 deaths reported annually (Erlanger et al., 2009; Solomon, 2004). In severe cases, JEV crosses blood-brain barrier and induces acute encephalitis characterized as headache, high fever, vomiting, disorientation, coma, and ultimately death (Gwon et al., 2020; Misra and Kalita, 2010). ZIKV has garnered attention due to the explosive outbreak from 2014 to 2016. After detection in Brazil in late 2014, ZIKV has spread unprecedentedly in

Central and South America, Caribbean, Pacific Islands, and Southeast Asian countries, and infected millions of people (Lowe et al., 2018). ZIKV infection is usually associated with mild clinical manifestations including fever, rash, pain in joints, and conjunctivitis. In severe cases of ZIKV infection, neurological disorders like microcephaly and Guillain-Barré syndrome were reported in infants and adults, respectively (Saiz and Martín-Acebes, 2017). Due to the global transmission and increased ZIKV-associated microcephaly cases, the World Health Organization (WHO) declared a Public Health Emergency of International Concern in February 2016 (World Health Organization, 2016).

Despite the burden of flavivirus infections, no approved antiviral is available, and current therapeutic strategies are generally based on symptomatic treatment using anti-pyretics, analgesics, and anti-inflammatory drugs (Imran et al., 2019; Pierson and Diamond, 2020). Although safe and effective licensed vaccines exist, outbreaks still occur, highlighting challenges in executing effective control measures (DeWald et al., 2020; Mercorelli et al., 2018). Many countries remain at high risk of flaviviruses outbreaks due to worldwide trading and traveling, and the prevalence of vectors. Due to the global threat of flavivirus infections, there is an urgent need to develop antiviral drugs using novel approaches to control flavivirus infections. Dehydroepiandrosterone (DHEA) is one of the most abundant naturally occurring endogenous steroids in human blood, produced by various tissues, e.g. adrenal cortex, gonads, gastro-intestinal tract (GIT), and brain, and is further metabolized to sex steroid hormones (Dalla Valle et al., 1995; Majewska et al., 1990). DHEA has been proved to be effective in the treatment of immune disorders, viral infections, and cancer, but its usage for an extended period leads to increased circulating testosterone and dihydrotestosterone in females resulting in masculinization (Bradley et al., 1995). Several investigations found out DHEA analogs possessed beneficial effects and would not transform to sex hormones. These analogs have been used in various studies as a therapeutic agent (Coleman et al., 1982).

This study aimed to evaluate and characterize the *in vitro* antiviral activity of synthetic analogs of DHEA against JEV and ZIKV on different events of viral replication in Vero cell line as a model to ascertain their possible mode of action.
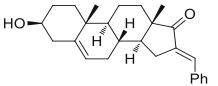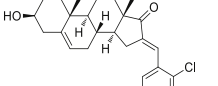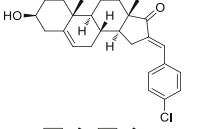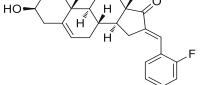
2. Materials and methods
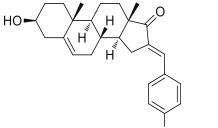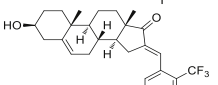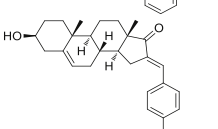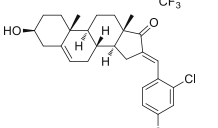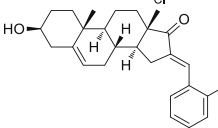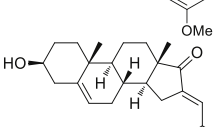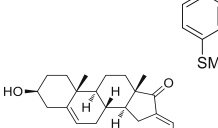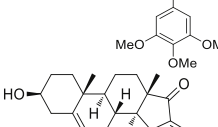
2.1. Cell culture and viruses

African green monkey kidney cells (Vero, ATCC-CCL-81), baby hamster kidney fibroblast cells (BHK-21) and adenocarcinomic human alveolar basal epithelial cells (A549, ATCC CCL-185) were cultured and maintained in Dulbecco's modified Eagle's medium (DMEM, 2357141, Gibco™, Waltham, USA) supplemented by 10% fetal bovine serum (FBS, 11011-8611, Zhejiang tianhang biotechnology, Hangzhou, China), 100 U/mL penicillin, and 100 mg/mL streptomycin in 5% CO_2 incubator at 37 °C. The JEV P3 strain (GenBank: U47032.1) was stored in our laboratory, while ZIKV H/PF/2013 strain (GenBank: KJ776791) was kindly provided by Dr. Bo Zhang, Wuhan Institute of Virology, Chinese Academy of Sciences.

2.2. Reagents

DHEA derivatives were prepared in our laboratory as reported previously (Ke et al., 2013). A stock solution was prepared in dimethyl sulfoxide (DMSO) with a concentration of 10 mmol/L. Further dilutions of this stock solution were prepared in DMEM prior to performing biological experiments. The structure of DHEA derivatives was shown in Table 1. The monoclonal antibodies (mAb) against ZIKV (E, NS5) and JEV (E, NS5) were generated in our laboratory. Anti-mouse and anti-rabbit IgG secondary antibody conjugated with horse reddish peroxidase were purchased from Boster (BST16B20B16B51, Wuhan, China).

Table 1
Synthetic analogs of DHEA.

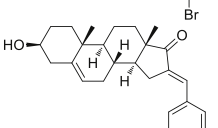| Sample number	Compound number	Structure	Molecular weight (g/mol)
1	HAAS-AV3001		376.2
2	HAAS-AV3002		410.2
3	HAAS-AV3003		410.2
4	HAAS-AV3004		394.2
5	HAAS-AV3005		394.2
6	HAAS-AV3006		444.2
7	HAAS-AV3007		444.2
8	HAAS-AV3008		444.2
9	HAAS-AV3009		472.1
10	HAAS-AV3010		406.3
11	HAAS-AV3011		422.2
12	HAAS-AV3012		466.3
13	HAAS-AV3013		377.2

Table 1 (*continued*)

Sample number	Compound number	Structure	Molecular weight (g/mol)
14	HAAS-AV3014		377.2
15	HAAS-AV3015		377.2
16	HAAS-AV3016		468.3
17	HAAS-AV3017		415.3
18	HAAS-AV3018		449.2
19	HAAS-AV3019		449.2
20	HAAS-AV3020		433.3
21	HAAS-AV3021		433.3
22	HAAS-AV3022		483.2
23	HAAS-AV3023		483.2
24	HAAS-AV3024		483.2
25	HAAS-AV3025		511.2

Table 1 (*continued*)

Sample number	Compound number	Structure	Molecular weight (g/mol)
26	HAAS-AV3026		445.3
27	HAAS-AV3027		461.3
28	HAAS-AV3028		505.3
29	HAAS-AV3029		416.3
30	HAAS-AV3030		416.3
31	HAAS-AV3031		416.3
32	HAAS-AV3032		507.3

2.3. Cell viability assay and efficacy study of DHEA derivatives

Cell Titer-GLO® One Solution Assay kit (G7572, Promega, Madison, USA) was used for cell viability assay (Imran et al., 2019). This assay quantitates ATP of cells which ultimately indicates cultured cell viability. Briefly, BHK-21 and Vero cells were seeded in a 96-well plate. After 24 h, cell culture supernatants were replaced with different concentrations of DHEA derivatives or DMSO and tested in triplicates. A mixture of 100 μL of phosphate-buffered saline (PBS) and 100 μL of Cell Titer-GLO® reagent was used to wash cells after 72 h. For complete lysis of the cells, a 96-well plate was agitated on a shaker for 2 min and was then placed at room temperature for 10 min. After that, luminescence signals were quantitated using a Multimode plate reader (BMG LABTECH, Ortenberg, Germany) and then compared the luminescence value with its corresponding DMSO control. The data of cell viability assay were used to determine the median cytotoxic concentration (CC_{50}) of DHEA derivatives by non-linear regression model using GraphPad Prism (version 7) software.

The efficacy of DHEA derivatives against JEV and ZIKV (0.1 MOI) was studied by using various concentrations of hits (1, 10, 50, and 100 μmol/L) after 24 h post-infection (hpi) by plaque reduction assay. The results were used to determine half maximal inhibitory concentration (IC_{50}) of DHEA derivatives by non-linear regression model using GraphPad Prism (version 7) software.

2.4. Immunofluorescence assay (IFA)

Vero cells infected by JEV (0.1 MOI) or ZIKV (0.1 MOI) were treated with DHEA derivatives or DMSO and were then fixed after a specific time

point with ice-cold methanol for 10 min. After washing with PBS, cells were blocked with 10% bovine serum albumin (BSA) in PBS for 30 min at room temperature. Later, cells were treated with a primary antibody, mouse polyclonal anti-NS5 of JEV or ZIKV for 1 h at room temperature. After that, cells were washed with PBS and incubated with a secondary antibody (Alexa Fluor 488, 2284614, Invitrogen, Waltham, USA) for 30 min at room temperature. To stain cell nuclei, 6-diamidino-2-phenyl indole (DAPI, 2116139, Invitrogen) was used. The cells were observed under a fluorescence microscope (Zeiss, Invitrogen) (Ashraf et al., 2016; Zhu et al., 2015).

2.5. Plaque assay

Viral titers in cells supernatant were determined as described in our previous study (Imran et al., 2019). Briefly, JEV- or ZIKV-infected Vero cells were treated with DHEA derivatives or DMSO. After a specific time point post-infection, virus-containing cell supernatants were serially diluted in DMEM and adsorbed on Vero monolayer for 1 h. Afterward, unbound viral particles in the medium were removed and overlaid with 2% carboxy methyl cellulose (CMC). After five days of incubation, cells were fixed with 10% formaldehyde for 12 h and were then stained with 0.1% crystal violet for 6 h. The visible plaques were counted and viral loads were measured as a plaque-forming unit (PFU) per mL of supernatant. All data are expressed as the means of triplicate samples (Chen et al., 2016).

2.6. Time-of-drug addition assay

Vero cells infected by ZIKV (0.1 MOI) and JEV (0.1 MOI) were treated with DHEA derivatives under the following conditions: 1 h before infection, at the time of infection, or 1, 6, and 12 hpi. Regardless of treatment time, cells were infected for 1 h. After 1 h, infectious medium was replaced with fresh medium, and DHEA derivatives were added according to the above time points. Supernatants were collected at 24 hpi to determine viral titer by plaque assay (Imran et al., 2019).

2.7. Viral attachment and entry assay

In viral adsorption or attachment assay, the effect of DHEA derivatives on virus receptors was investigated. ZIKV or JEV (10^5 PFU, 5 MOI) with DHEA derivatives (5 μmol/L) were added to Vero cells at 4 °C for 1 h to allow viral adsorption. After incubation, cells were washed and the medium was replaced with DMEM containing 2% FBS. After 1 h of incubation at 37 °C, samples were collected to detect the virus titer by plaque assay.

In viral entry assay, Vero cells were infected with ZIKV or JEV (5 MOI) and were incubated at 4 °C for virus attachment. After 1 h of incubation, unbound infected particles were washed and the medium was replaced with fresh media containing DHEA derivatives (5 μmol/L). After 1 h of incubation at 37 °C, the temperature was shifted from 4 °C to 37 °C to promote virus entry. After 1 h, cells were washed by cold alkaline-high-salt solution (1 mol/L NaCl and 50 mmol/L sodium bicarbonate, pH 9.5) to remove free virus, and then the media was replaced with DMEM containing 2% FBS. After placed in incubator at 37 °C for 1 h, samples were collected to detect the virus titer by plaque assay (Fan et al., 2016).

2.8. JEV replicon assay

To ensure the effectiveness of the compound on JEV replication, the JEV replicon cDNA clone in which the structural genes were replaced with the Renilla luciferase (Rluc) gene was employed to quantitatively evaluate the inhibitory effects. In vitro transcripts were synthesized from linearized JEV replicon using a T7 mMessage mMachine kit (00762139, Invitrogen) according to the manufacturer's instructions and were then transfected into BHK-21 cells. After transfection, the cells were plated in

DMEM supplemented with 10% FBS, and compounds were added to the medium when specified. At the indicated times post-transfection, the cells were harvested, and luciferase activity was measured using the Rluc assay system (0000404583, Promega) (Guo et al., 2020).

2.9. Western blot analysis

Cells were lysed using radioimmunoprecipitation assay (RIPA) buffer (R0278, Sigma, St. Louis, USA) containing protease inhibitor (C0001, Roche, targetmol, Boston, USA). Samples were mixed with loading buffer, heated at 95 °C for 10 min and were then fractionated by SDS-PAGE. Proteins were transferred to a polyvinylidene fluoride membrane (Millipore) by using Mini Trans-Blot Cell (Bio-Rad, Hercules, USA) and blocked with 1% BSA. Blots were probed with relevant primary and secondary antibodies. The monoclonal antibodies (mAb) against ZIKV (E, NS5) and JEV (E, NS5) were generated in our laboratory. Anti-mouse and anti-rabbit IgG secondary antibody conjugated with horse reddish peroxidase were purchased from Boster (BST16B20B16B51). Proteins were detected by enhanced chemiluminescent reagent (Tanon-4600, Tanon, shanghai, China) (Zhu et al., 2016).

2.10. RNA extraction and quantitative real-time PCR

Total cellular RNA was obtained using TRIzol Reagent (213501, Ambion, Austin, USA), and reverse transcription of RNA was performed with a first-strand cDNA synthesis kit (RK20400, Abclonal, Wuhan, China), according to the manufacturer's instructions. qRT-PCR was performed using the QuantStudio 6 Flex PCR system (Thermo Fisher Scientific, Waltham, USA) and SYBR green PCR master mix (RK21203, Abclonal). The results were normalized to the endogenous expression of β-actin in each sample (Wan et al., 2016). Primers were as follows: ZIKV-NS5, 5′-TAAACGGGGTTG TCAGGCTC-3′ (forward) and 5′-ACCTGACGAGTGCCTTCTTG-3′ (reverse); JEV-C, 5′-GGCTCTTATCACGTTCTTCAAGTTT-3′ (forward) and 5′-TGCTTTCCATCGGCCYAAAA-3′ (reverse); human β-actin, 5′-CTCCATCC TGGCCTCGCTGT-3′ (forward) and 5′-GCTGTCACCTTCACCGTTC-3′ (reverse).

2.11. Statistical analysis

All experiments were performed at least three times with similar conditions. GraphPad Prism (version 7) was used for data analyses of outcomes. Results are presented as mean ± standard error (SEM). CC_{50} and IC_{50} were calculated by non-linear regression. Viral titers are expressed as the mean ± standard deviation (SD). Statistical differences were determined by independent t-test or one-way analysis of variance (ANOVA) with Dunnett's post-test, and a P value < 0.05 was considered significant.

3. Results

3.1. Screening of potential DHEA derivatives against JEV infection

Plaque reduction assay based screening was conducted using 32 compounds at a final concentration of 10 μmol/L on JEV-infected (0.1 MOI) BHK-21 cells to identify potent antiviral compounds (Fig. 1). Viral titers in treated and untreated culture medium were determined after 24 hpi. Compounds that exhibited a more significant reduction of JEV infection compared with parent DHEA were arbitrarily considered as hits. These compounds named as HAAS-AV3023, HAAS-AV3024, HAAS-AV3025, HAAS-AV3026, HAAS-AV3027, and HAAS-AV3028 (Fig. 1).

3.2. Cytotoxicity assessment of hits

HAAS-AV3023, HAAS-AV3024, HAAS-AV3025, HAAS-AV3026, HAAS-AV3027, and HAAS-AV3028 were then subjected to cell viability assay to validate their anti-JEV activity was not due to cell toxicity. A
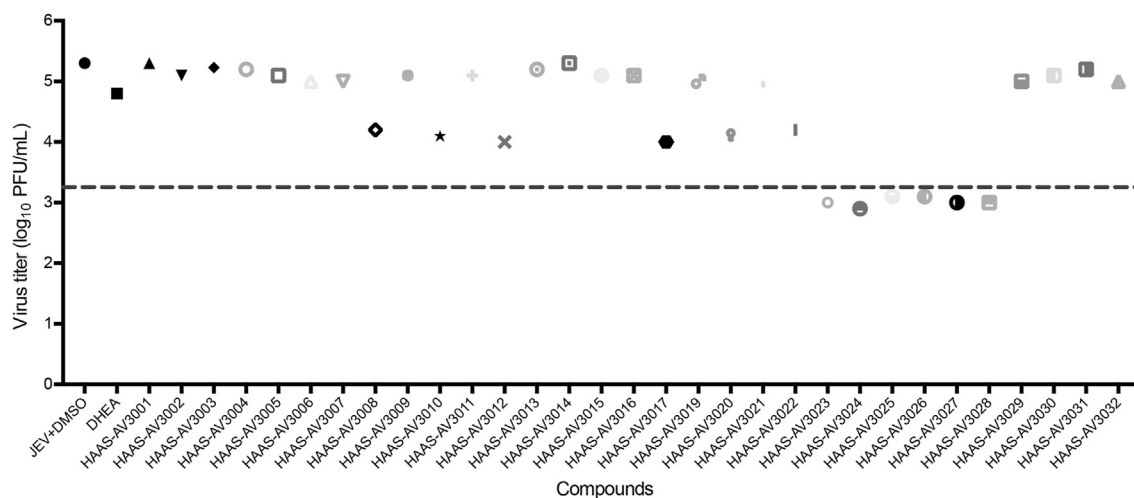
Fig. 1. Screening of DHEA synthetic analogs as antivirals against JEV. BHK-21 cells were infected with JEV (0.1 MOI) and were incubated with 10 μmol/L of DHEA synthetic derivatives for 24 h. Then, supernatants were harvested and were subjected to plaque assay to determine cell-free virus yields. DHEA, Dehydroepiandrosterone; JEV, Japanese encephalitis virus; MOI, multiplicity of infection.

Fig. 2. Determination of cytotoxicity of DHEA synthetic analogs. Cytotoxicity of the compounds in BHK-21 cells (**A–F**) and Vero cells (**G–I**) were tested using a luminescence-based cell viability assay. Cell viability values were used to determine CC_{50} by non-linear regression analysis through GraphPad Prism. DHEA, Dehydroepiandrosterone; CC_{50}, 50% cytotoxic concentration.

Fig. 3. DHEA derivative hits inhibit JEV and ZIKV in a dose-dependent manner. Vero cells were infected with JEV or ZIKV (0.1 MOI) and were treated with increasing concentra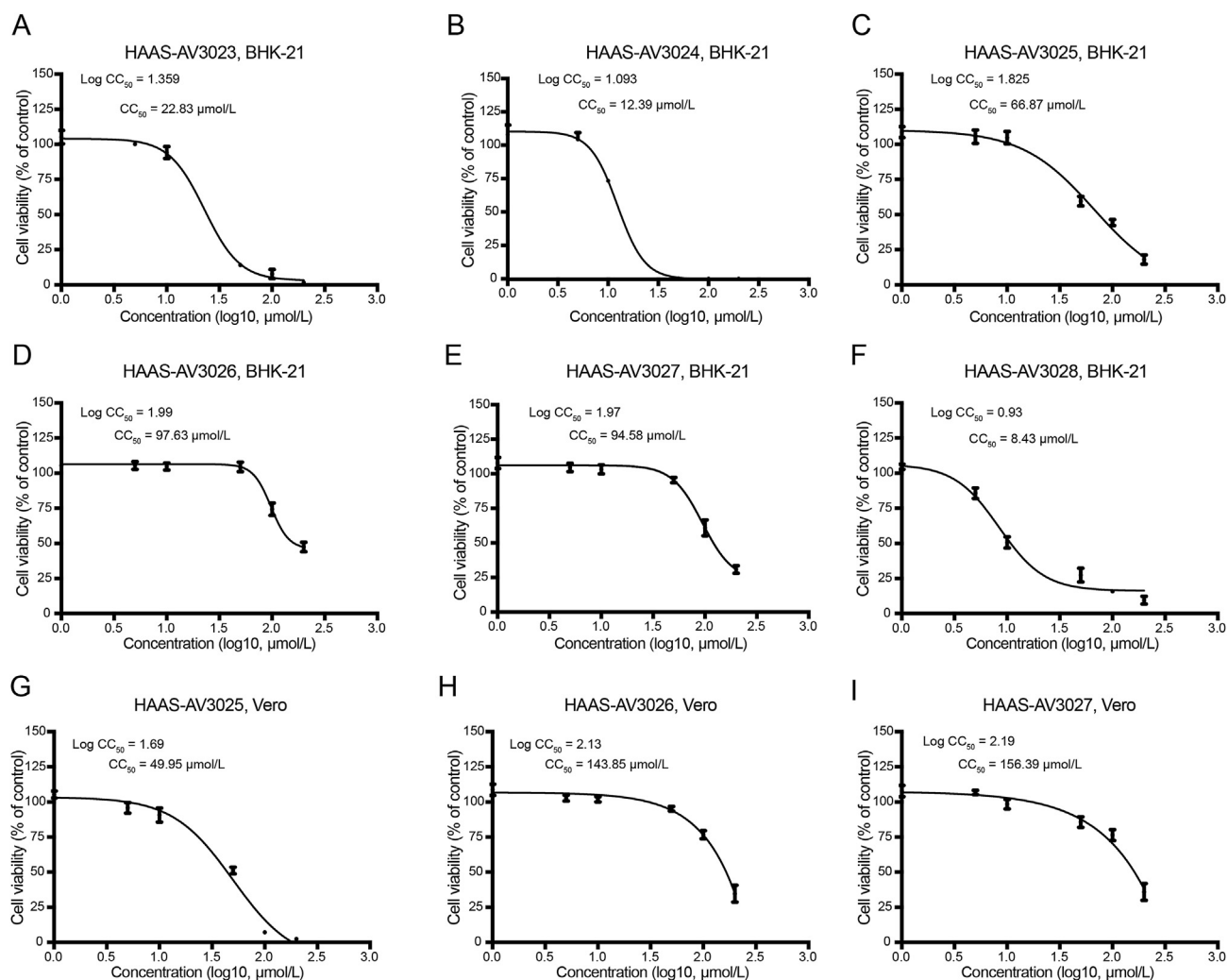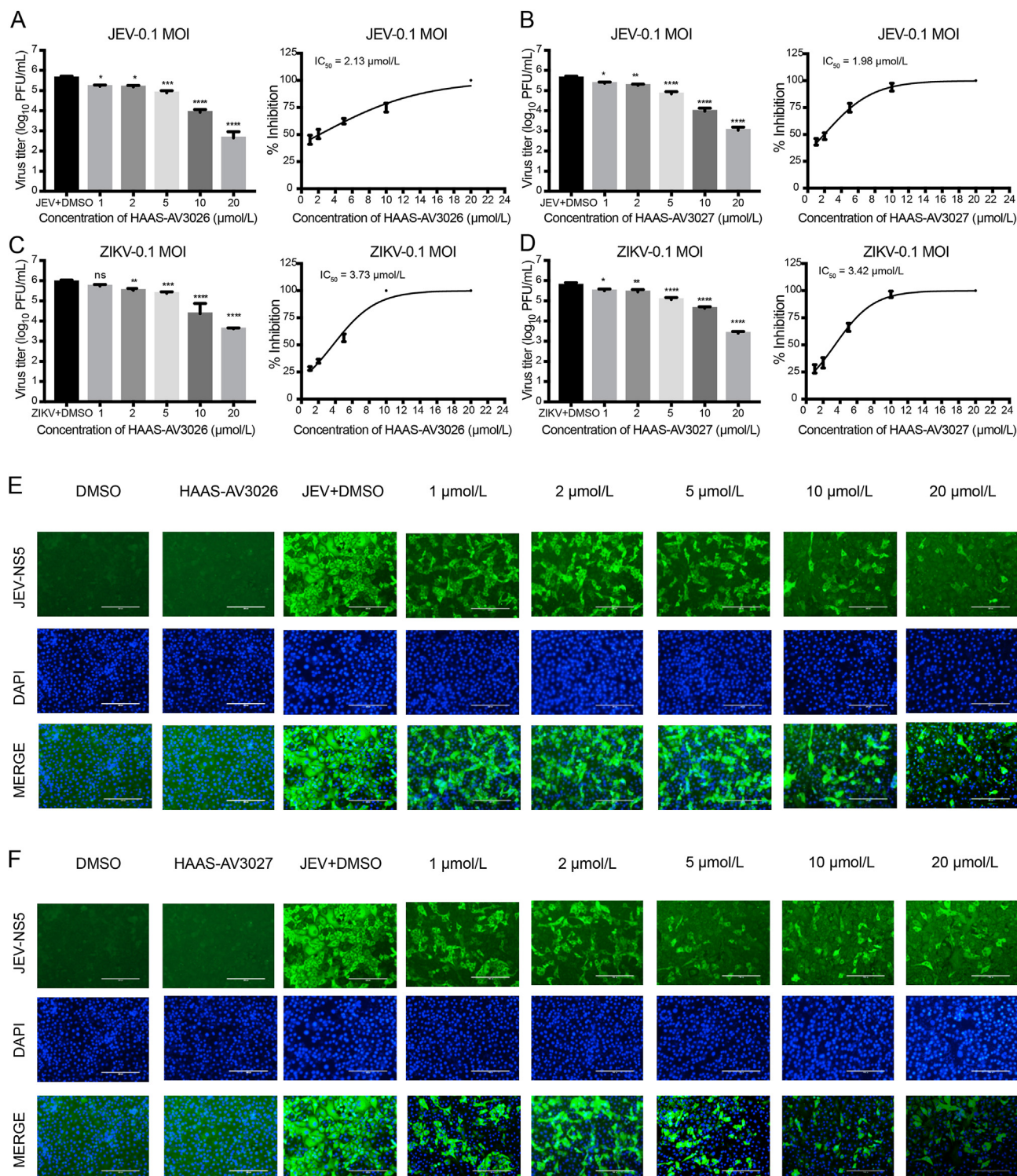tions of both HAAS-AV3026 and HAAS-AV3027. Supernatants were harvested at 24 hpi to determine virus titers by plaque assay. Right panels indicate virus titers while left panels indicate IC_{50} of hits against JEV (**A** and **B**) and ZIKV (**C** and **D**). Infected cells with similar conditions were fixed to analyze JEV (**E** and **F**) and ZIKV (**G** and **H**) spreading from infected to neighboring cells by IFA. Scale bar = 200 μm. Cytotoxicity of hits against A549 cell line was determined by CellTiter-GLO One Solution Assay kit (Promega) (**I** and **J**). A549 cells were infected with JEV or ZIKV (0.1 MOI) and were treated with increasing concentrations of both HAAS-AV3026 and HAAS-AV3027. Supernatants were harvested at 24 hpi to determine virus titers of both JEV (**K** and **L**) and ZIKV (**M** and **N**) by plaque assay respectively. IC_{50} was calculated by non-linear regression analysis. Statistical analysis was performed using one-way ANOVA, followed by Dunnett's multiple comparisons test. *$P < 0.05$, **$P < 0.01$, ***$P < 0.001$, ****$P < 0.0001$. Data are presented as the mean ± standard deviation (SD) for three independent experiments. DHEA, Dehydroepiandrosterone; JEV, Japanese encephalitis virus; ZIKV, Zika virus; MOI, multiplicity of infection; hours post-infection; IC_{50}, half-maximal inhibitory concentration; IFA, immunofluorescence assay; ns, non-significant.

Fig. 3. (*continued*).

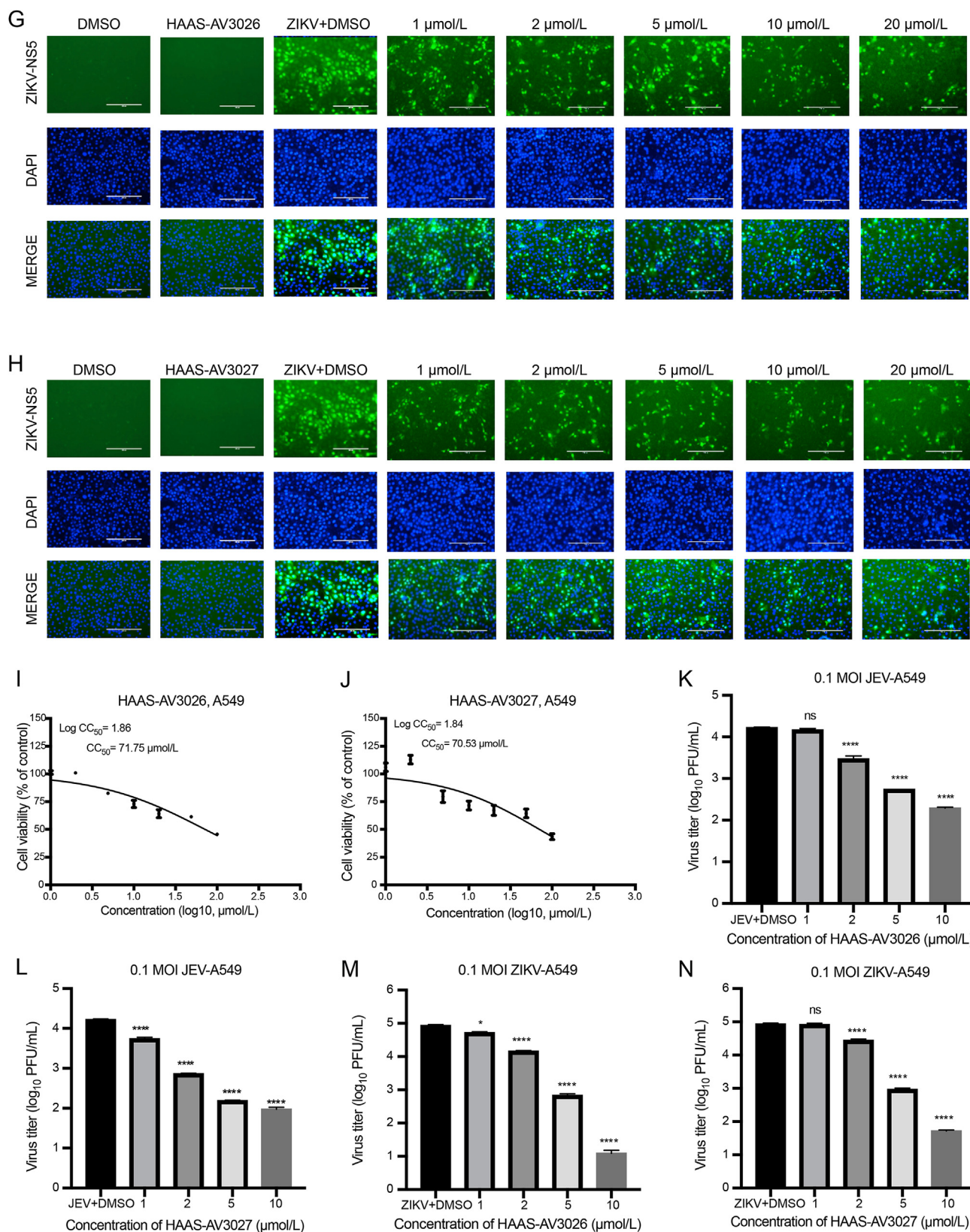luminescence-based cell viability assay was conducted to examine the cytotoxicity of hits using different concentrations on BHK-21 cells. Viable cells were quantified based on ATP level, which indicated the presence of metabolically active cells. As shown in Fig. 2C–E, the CC_{50} of HAAS-AV3025, HAAS-AV3026, and HAAS-AV3027 was 66.87, 97.63, and 94.58 μmol/L, respectively. HAAS-AV3023, HAAS-AV3024, and HAAS-

AV3028 showed lower CC_{50} values (22.83, 12.39, and 8.43 µmol/L, respectively) (Fig. 2A, B, and 2F). Furthermore, HAAS-AV3026 and HAAS-AV3027 displayed higher CC_{50} on Vero cells (Fig. 2G, H, and 2I). Based on the results of plaque assay and cytotoxicity, HAAS-AV3026 and HAAS-AV3027 were chosen as the lead compound for downstream study.

3.3. HAAS-AV3026 and HAAS-AV3027 suppresses JEV and ZIKV propagation in a dose-dependent manner

Next, we measured antiviral effect of HAAS-AV3026 and HAAS-AV3027 against flaviviruses at five different doses. JEV- and ZIKV-infected Vero cells were subjected to increasing concentration of the hits, followed by plaque assay to determine the viral titer. Meanwhile, cells were fixed for indirect immunofluorescence assay to observe virus propagation inside the cells. As shown in Fig. 3A and B, HAAS-AV3026 and HAAS-AV3027 suppressed JEV replication in a dose-dependent manner (IC_{50} = 2.13 and 1.98 µmol/L, respectively). Similar effect was observed as for ZIKV (Fig. 3C and D). The IC_{50} of HAAS-AV3026 and HAAS-AV3027 against ZIKV was 3.73 and 3.42 µmol/L, respectively.

To perceive the effect of hits on intracellular virus particles, immunofluorescence images of JEV- and ZIKV-infected cells with or without treatment were taken at 24 hpi. In JEV-infected cells, fluorescence signals

were reduced after treatment of increasing concentration of HAAS-AV3026 or HAAS-AV3027, compared to control groups (Fig. 3E and F). Similar results were also observed in ZIKV-infected cells (Fig. 3G and H). Taken together, the data suggested that HAAS-AV3026 and HAAS-AV3027 inhibited JEV and ZIKV replication in a dose-dependent manner.

To address whether HAAS-AV3026 and HAAS-AV3027 inhibit JEV and ZIKV infections in human cell line, we examined the cytotoxicity of hits on A549 cells firstly by luminescence-based cell viability assay and then measured the antiviral effect of the hits against flaviviruses by plaque assay. The CC_{50} of HAAS-AV3026 and HAAS-AV3027 on cell viability of A549 was 71.75 and 70.53 µmol/L, respectively (Fig. 3I and J). HAAS-AV3026 and HAAS-AV3027 showed dose-dependent inhibitory effects against JEV and ZIKV in A549 cells (Fig. 3K–N). These results suggest that HAAS-AV3026 and HAAS-AV3027 also inhibit ZIKV and JEV propagation in human cell line (A549).

3.4. HAAS-AV3026 and HAAS-AV3027 inhibit JEV and ZIKV propagation at different MOIs and various time points

The anti-JEV and anti-ZIKV effect of both compounds were also investigated in Vero cells infected with different MOIs (0.1, 1, and 10) at 24 hpi. As shown in Fig. 4A and B, virus titers increased with increasing
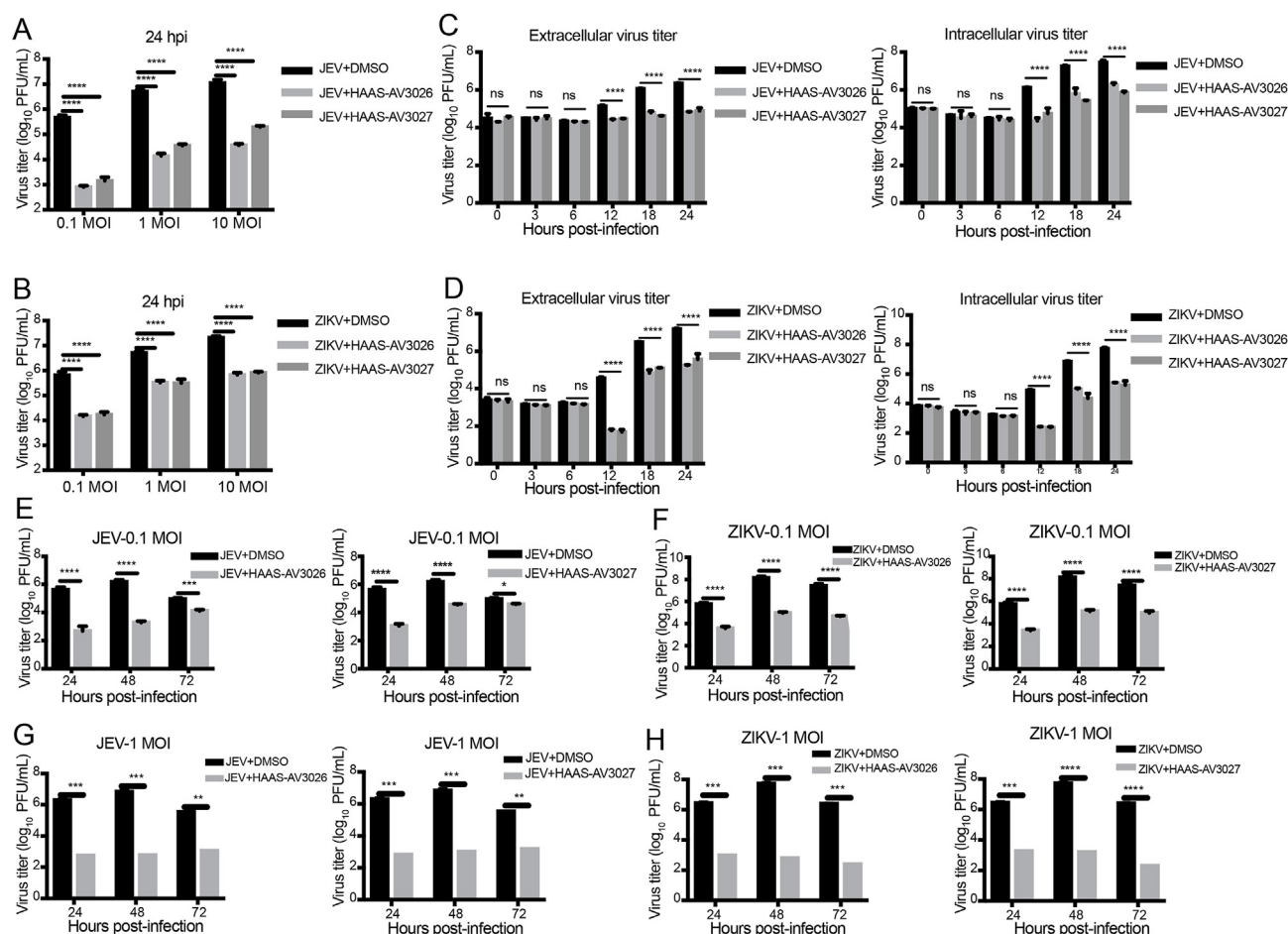

Fig. 4. Anti-JEV and ZIKV effect of DHEA analogs at different MOIs and their growth kinetics. Vero cells were infected with different MOI (0.1, 1, and 10) of JEV or ZIKV and were treated with 10 µmol/L of both HAAS-AV3026 and HAAS-AV3027. Supernatants were harvested at 24 hpi to determine JEV (**A**) and ZIKV (**B**) titers by plaque assay. For the one-step growth cycle, Vero cells were infected with JEV or ZIKV at an MOI of 5 for 1 h followed by DHEA analogs or 0.1% DMSO treatment after washing the cells. Supernatants and cells were collected at indicated time points. For the liberation of cells-associated virus particles, cells were subjected to three freeze-thaw cycles. After that, extracellular (left panel) and intracellular (right panel) JEV (**C**) and ZIKV (**D**) titers were determined by plaque assay. The inhibitory effect of HAAS-AV3026 (left panel) and HAAS-AV3027 (right panel) was also determined at multiple time points against 0.1 and 1 MOI of both JEV (**E** and **G**) and ZIKV (**F** and **H**) by using cell supernatants through plaque assay. Statistical analysis was performed using two-way ANOVA, followed by Dunnett's multiple comparisons test. *$P < 0.05$, **$P < 0.01$, ***$P < 0.001$, ****$P < 0.0001$. Data are presented as the mean ± SD for three independent experiments. JEV, Japanese encephalitis virus; ZIKV, Zika virus; DHEA, Dehydroepiandrosterone; MOI, multiplicity of infection; hpi, hours post-infection; SD, standard deviation; ns, non-significant.

MOIs in 0.1% DMSO-treated control cells, indicating that the experiment was carried out properly. Treatment of HAAS-AV3026 and HAAS-AV3027 (10 μmol/L) to JEV-infected cells exhibited strong inhibition against JEV infections at all MOIs (Fig. 4A). In the case of ZIKV infection, significant inhibition on virus propagation was also observed in treatment groups as compared to DMSO-treated vehicle control (Fig. 4B).

To obtain a detailed insight into the efficacy of HAAS-AV3026 and HAAS-AV3027 on JEV and ZIKV replication kinetics, a one-step curve was conducted on Vero cells. For this purpose, JEV- and ZIKV-infected (5 MOI) Vero cells were treated with 10 μmol/L of HAAS-AV3026 and HAAS-AV3027. Both cells and supernatants were harvested at 0, 3, 6, 12, 18, and 24 hpi and were subjected to plaque assay for viral titer determination. The data revealed that virus proliferation started between 6 and 12 hpi in vehicle-treated cells, and kept rising at 18 to 24 hpi. Treatment of HAAS-AV3026 and HAAS-AV3027 led to a significant reduction of virus titer in both of the extracellular and intracellular compartments of JEV-infected cells, compared to vehicle-treated cells (Fig. 4C). Similar findings were also observed in the case of ZIKV infections (Fig. 4D). Thus, these results indicate that HAAS-AV3026 and HAAS-AV3027 affect virus replication.

We also measured the antiviral efficacy of these compounds against JEV (0.1 and 1 MOI) and ZIKV (0.1 and 1 MOI) in Vero cells at a dose of 10 μmol/L after 24, 48, and 72 hpi. Cell supernatants were collected at indicated time points for determination of virus progeny titer through plaque assay. At an MOI of 0.1, treatment with HAAS-AV3026 and HAAS-AV3027 resulted in 2.97 and 2.9 log10 decrease in JEV titer at 24 hpi, 2.9 and 1.62 log10 at 48 hpi, and 0.8 and 0.36 log10 at 72 hpi respectively, compared to DMSO control (Fig. 4E). Similarly, in case of ZIKV, treatment with HAAS-AV3026 and HAAS-AV3027 at an of MOI resulted in 2.2 and 2.3 log10 decrease in virus titer at 24 hpi, 3.13 and 3.02 log10 at 48 hpi, and 2.8 and 2.4 log10 at 72 hpi respectively, compared to DMSO control (Fig. 4F).

Whereas, at an MOI of 1, treatment with HAAS-AV3026 and HAAS-AV3027 resulted in 3.6 and 3.5 log10 decrease in JEV titer at 24 hpi, 4.1 and 3.8 log10 at 48 hpi, and 2.5 and 2.3 log10 at 72 hpi respectively, compared to DMSO control (Fig. 4G). Similarly, in case of ZIKV,

treatment with HAAS-AV3026 and HAAS-AV3027 at an MOI of 1 resulted in 3.5 and 3.1 log10 decrease in virus titer at 24 hpi, 4.9 and 4.5 log10 at 48 hpi, and 4.1 and 3.5 log10 at 72 hpi respectively, compared to DMSO control (Fig. 4H).

3.5. HAAS-AV3026 and HAAS-AV3027 inhibit viral protein and RNA synthesis

To determine the effect of the compounds on protein synthesis, especially on E and NS5, JEV- and ZIKV-infected Vero cells (MOI = 5) were subjected to Western blot analysis after treatment with DHEA derivatives. The gray density of protein was quantified by image J software. Uninfected cells treated with 0.1% DMSO were used as a negative control. Meanwhile, infected cells treated with 0.1% DMSO were also included to rule out the negative effect of DMSO on the production of viral protein. GAPDH was used as a loading control in the experiment and also ensured that treatment of DHEA derivatives did not affect the expression of the housekeeping gene. As shown in Fig. 5A and B, treatment with HAAS-AV3026 and HAAS-AV3027 significantly reduced the expression of JEV-E and NS5 proteins at indicated time points as compared to JEV-infected and DMSO treated cells. In the case of ZIKV, similar inhibitory effects were also observed (Fig. 5C and D). These results suggest that HAAS-AV3026 and HAAS-AV3027 inhibit JEV ZIKV protein production, which can explain the decrease in virus titers observed in plaque assays. Subsequently, qRT-PCR was performed to evaluate the antiviral effect of hits on viral RNA synthesis in JEV- and ZIKV-infected cells (MOI = 5) at different time points. Viral RNA copies in infected cells treated with 0.1% DMSO were served as vehicle control. The expression level of mRNA was normalized to the reference β-actin gene. Based on qRT-PCR findings, treatment with HAAS-AV3026 and HAAS-AV3027 significantly inhibited the expression of JEV mRNA at 12, 18, and 24 hpi as compared to vehicle control (Fig. 5E). Similar findings were also observed in the case of ZIKV, where both compounds significantly reduced viral RNA synthesis at 12, 18, and 24 hpi as compared to vehicle control (Fig. 5F). These results suggest that hits of DHEA derivatives attenuate JEV and ZIKV viral RNA synthesis.
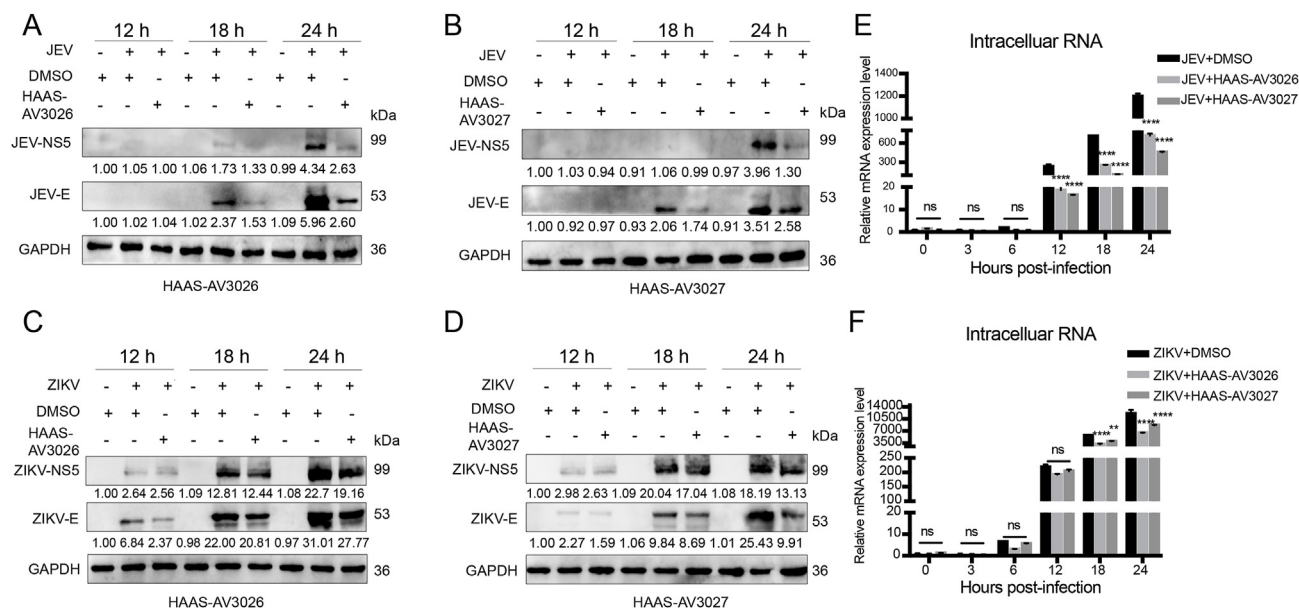

Fig. 5. Antiviral effects of DHEA analogs against viral protein and RNA synthesis. Vero cells were infected with JEV (**A** and **B**) or ZIKV (**C** and **D**) at an MOI of 5 and were treated with 10 μmol/L of HAAS-AV3026 or HAAS-AV3027. Samples were collected at indicated time points. Western blot analyses were conducted to determine antiviral effects of HAAS-AV3026 and HAAS-AV3027 on protein level. The gray intensity of protein was quantified by image J software. qRT-PCR was also performed to measure the effects on RNA synthesis of JEV (**E**) and ZIKV (**F**). The results were normalized to the endogenous expression of β-actin in each sample. Statistical analysis was performed using two-way ANOVA, followed by Dunnett's multiple comparisons test. *$P < 0.05$, **$P < 0.01$, ***$P < 0.001$, ****$P < 0.0001$. Data are presented as the mean ± SD for three independent experiments. DHEA, Dehydroepiandrosterone; JEV, Japanese encephalitis virus; ZIKV, Zika virus; MOI, multiplicity of infection; ns, non-significant; SD, standard deviation.

3.6. HAAS-AV3026 and HAAS-AV3027 inhibit JEV and ZIKV infection at different times of drug administration

Time-addition assay was performed to find the window in JEV and ZIKV replication cycle where HAAS-AV3026 and HAAS-AV3027 worked more effectively. For this purpose, JEV- and ZIKV-infected Vero cells were treated with 10 μmol/L of HAAS-AV3026 and HAAS-AV3027 at various time points, i.e. 1 h before infection, at the time of infection, and three-time points post-infection (1, 6, and 12 hpi). Supernatants were harvested at 24 hpi and were subjected to plaque assay for virus titer determination.

In case of JEV, decreased virus titer was observed at the time of co-administration of drug and virus into the cells and treatment after infection as compared to DMSO-treated control. HAAS-AV3026 caused 1.1 log10 JEV titer reductions at the time of co-administration, while 2.9, 2.5, and 2.4 log10 reduction after 1, 6, and 12 hpi respectively (Fig. 6A). Similarly, HAAS-AV3027 caused 1.05 log10 JEV titer reductions at the time of co-administration, while 2.3, 2.17, and 1.98 log10 reduction after 1, 6, and 12 hpi respectively (Fig. 6B).

In case of ZIKV, HAAS-AV3026 caused 0.36 log10 reduction in virus titer at pre-infection treatment, 0.9 log10 reduction at the time of co-administration, while 2.9, 2.5, and 2.4 log10 reduction after 1, 6, and 12 hpi respectively (Fig. 6C). Similarly, HAAS-AV3027 caused 0.35 log10 reduction in virus titer at pre-infection treatment, 0.9 log10 JEV titer reduction at the time of co-administration, while 2.2, 1.86, and 1.78 log10 reduction after 1, 6, and 12 hpi respectively (Fig. 6D).

3.7. HAAS-AV3026 and HAAS-AV3027 inhibit JEV and ZIKV infection at the replication stage

Minimal inhibitory effects on virus propagation at pre-infection and co-administration treatments stage enlighten us to investigate whether HAAS-AV3026 and HAAS-AV3027 affect the early stage of the flavivirus replication cycle. For this purpose, viral adsorption/binding and entry assays were performed to determine the interaction of drugs with host cell receptors. As seen in Fig. 7A and B, no significant difference was observed in JEV and ZIKV titer for treated cells as compared to vehicle control cells, indicating the compounds showed no effect on flavivirus binding. In viral entry assay, chloroquine was used as positive control. Similar results of DHEA derivative hits were observed on flavivirus entry, while chloroquine significantly inhibited both JEV and ZIKV entry into the cells (Fig. 7C and D). Thus, the results of time-addition assay may indicates that HAAS-AV3026 and HAAS-AV3027 exhibit no effect on flavivirus binding and entry process while significantly inhibit the post entry process, suggesting viral replication may be the main targeted stage of these compounds.

To confirm this hypothesis, BHK-21 cells were transfected with JEV replicon and were then treated with 10 μmol/L of HAAS-AV3026 and HAAS-AV3027. Afterward, luciferase activities were determined. Significant reduction of luciferase signals was observed at 24 h post-transfection (Fig. 7E), which ultimately indicated that both HAAS-AV3026 and HAAS-AV3027 inhibited flavivirus infection at the replication stage.
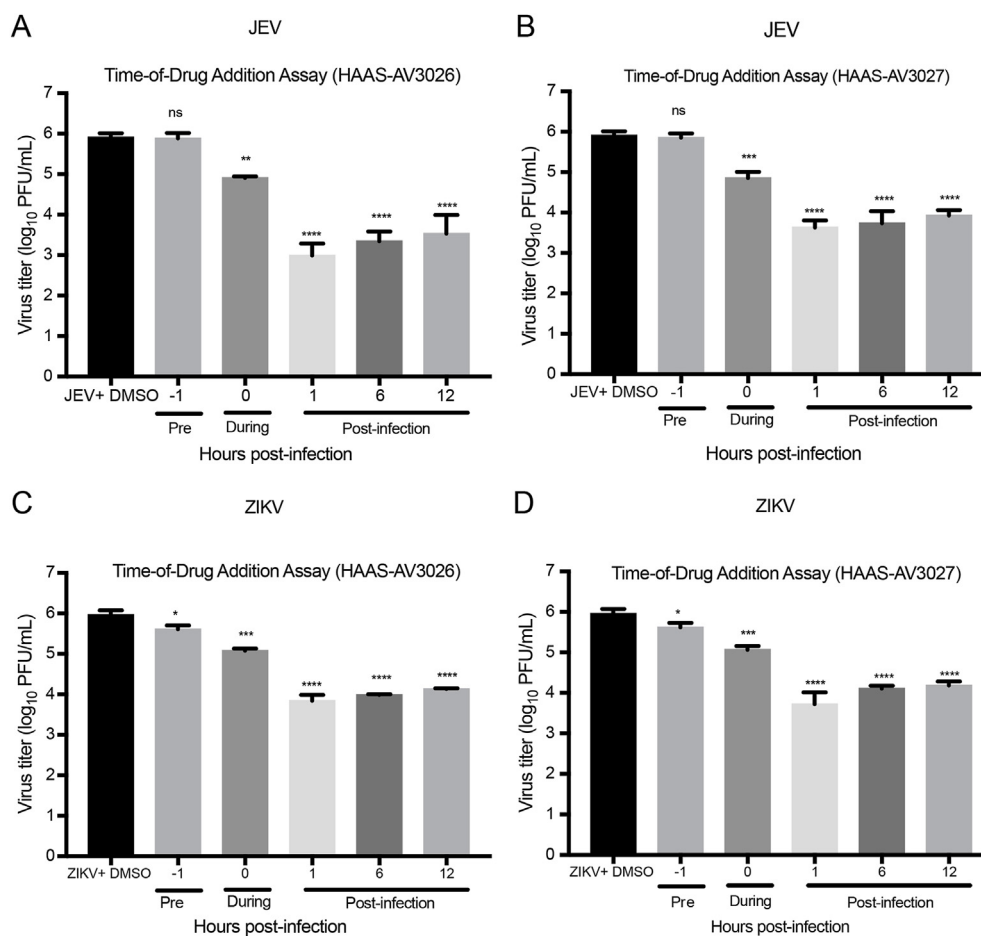

Fig. 6. Time-addition studies of DHEA derivative hits against JEV and ZIKV. Vero cells were infected with JEV or ZIKV (0.1 MOI) and treated with 10 μmol/L of both HAAS-AV3026 and HAAS-AV3027 at indicated time points. Cells supernatants were harvested at 24 hpi to determine JEV (**A** and **B**) and ZIKV (**C** and **D**) titers by plaque assay. Statistical analysis was performed using one-way ANOVA, followed by Dunnett's multiple comparisons test. *$P < 0.05$ **$P < 0.01$ ***$P < 0.001$ ****$P < 0.0001$. Data are presented as the mean ± standard deviation (SD) for three independent experiments. DHEA, Dehydroepiandrosterone; JEV, Japanese encephalitis virus; ZIKV, Zika virus; MOI, multiplicity of infection; hpi, hours post-infection; ns, non-significant.
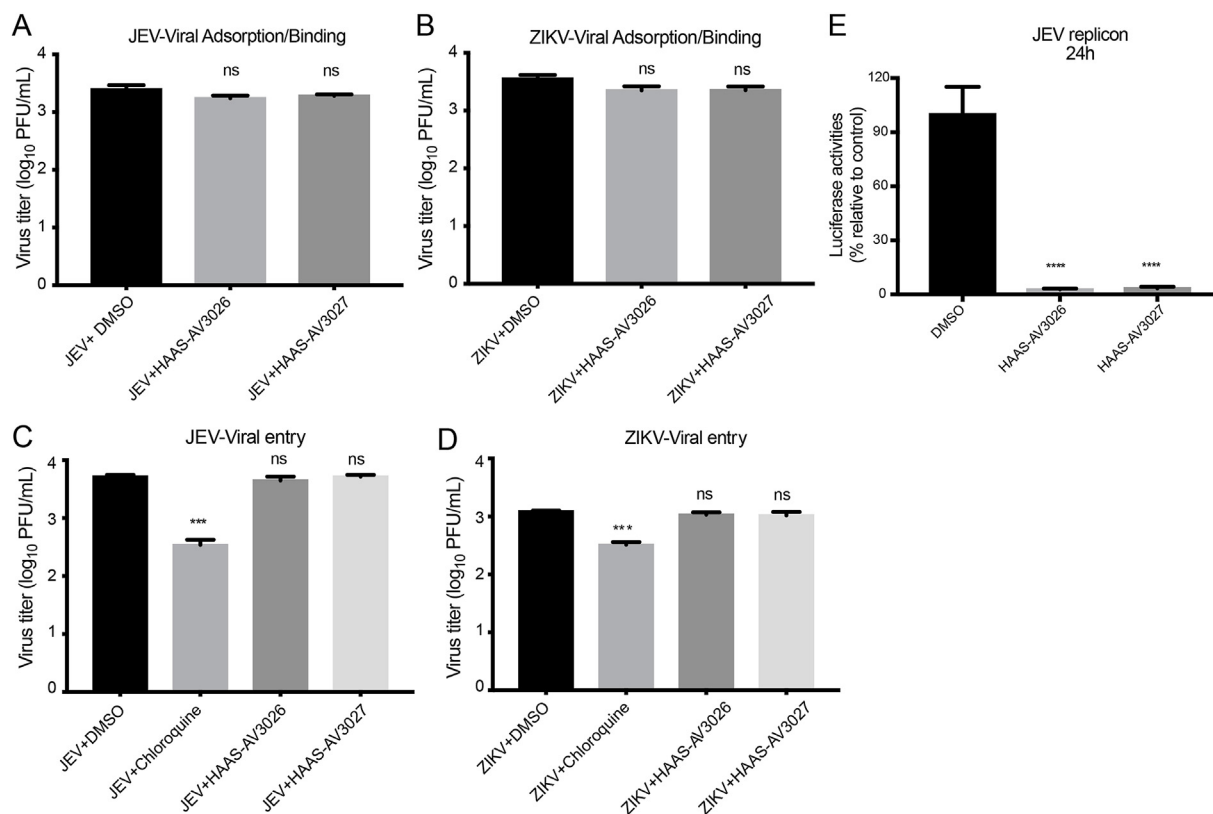
Fig. 7. Effects of DHEA derivative hit on JEV and ZIKV binding and entry assay. In the binding assay, JEV (10^5 PFU) or ZIKV (10^5 PFU) with DHEA derivative hits (10 μmol/L) were added to Vero cells at 4 °C for 1 h to allow viral adsorption. After incubation, cells were washed and medium was replaced with 2% FBS DMEM and put at 37 °C. JEV (**A**) and ZIKV (**B**) titers were determined by plaque assay. In the entry assay, JEV- or ZIK-infected (5 MOI) Vero cells were incubated at 4 °C for virus attachment. After 1 h of incubation, unbound infected particles were washed and replaced with medium containing DHEA derivative hits (10 μmol/L) or chloroquine (20 μmol/L), and then placed at 37 °C for 1 h. The temperature was shifted from 4 °C to 37 °C to promote virus entry. After 1 h, cells were washed and replenished with 2% FBS DMEM and put at 37 °C. After that, JEV (**C**) and ZIKV (**D**) titers were determined by plaque assay. BHK-21 cells were transfected with JEV replicon and were then treated with 10 μmol/L of DHEA derivative hits followed by determination of luciferase activities at different time points (**E**). Statistical analysis was performed using one-way ANOVA, followed by Dunnett's multiple comparisons test. $*P < 0.05$, $**P < 0.01$, $***P < 0.001$, $****P < 0.0001$. Data are presented as the mean $\pm$ SD for three independent experiments. DHEA, Dehydroepiandrosterone; JEV, Japanese encephalitis virus; ZIKV, Zika virus; MOI, multiplicity of infection; FBS, fetal bovine serum; ns, non-significant.

4. Discussion

Flaviviruses have been considered as a serious threat to global health which cause millions of infections annually (Laureti et al., 2018). Despite the existence of licensed vaccines, recent attempts to overcome these infections have failed, and it is uncertain whether new vaccination programs will be successful to control future outbreaks of flaviviruses. This issue has been emphasizing an urgent need for antiviral intrusions. Therefore, this study was conducted to fulfill this gap, which might provide a basis for the development of new antivirals against flaviviruses.

In the present work, a plaque assay-based primary screening of DHEA derivatives against JEV was conducted to find out the potent antiviral compounds. DHEA is a naturally occurring steroid in human blood and is mainly produced in the adrenal gland. However, persistent administration of DHEA leads to masculinization in women (Labrie et al., 2003). Previous studies have shown structural analogs of DHEA, which were used as potential therapeutic agents against human immunodeficiency virus 1, feline immunodeficiency virus, Junin virus, coxsackie B virus, herpes simplex type 2, vesicular stomatitis virus, JEV, and influenza virus (Acosta et al., 2008; Daigle and Carr, 1998; Pedersen et al., 2003).

From primary screening, two analogs HAAS-AV3026 and HAAS-AV3027 displayed strong antiviral activity against JEV and ZIKV at non-cytotoxic concentrations and also exhibited higher CC_{50} values both in BHK-21 and Vero cell lines, and were chosen as the lead compound for downstream studies. The CC_{50} values obtained from different cells varied

greatly, which indicated the different tolerant capacity. These findings were consistent with the results of chloroquine and hydroxychloroquine toxicity against multiple cell lines (Yang et al., 2020). In our study, higher CC_{50} value of DHEA derivative hits in BHK-21 as compared to Vero and A549 cell lines indicates the higher tolerant capacity of BHK-21.

A dose-dependent inhibition in JEV and ZIKV propagation was observed in terms of lowering extracellular virus titers and intracellular virus infection, yielding a selective index (SI = CC_{50}/IC_{50}) of 33.69 and 19.23 for HAAS-AV3026, while 35.62 and 20.62 for HAAS-AV3027 against JEV and ZIKV, respectively. Similar results were also reported for other analogs of DHEA against herpes simplex type 2 and vesicular stomatitis viruses (Romanutti et al., 2009). The anti-flaviviruses effect of DHEA derivatives was also found to be effective in inhibiting JEV and ZIKV propagation even at 72 hpi, which indicated that these derivatives had the potential of long-acting antiviral activity. Cumulatively, these results revealed that HAAS-AV3026 and HAAS-AV3027 would be safe and effective options against flaviviruses infections from a treatment point of view.

The antiviral efficacy of hits was also elucidated in a single round of flavivirus replication using a one-step growth cycle curve. A significant inhibition was found on virus proliferation. This inhibitory effect was similar in both intracellular and extracellular compartments of JEV- and ZIKV-infected Vero cells, which indicated that HAAS-AV3026 and HAAS-AV3027 showed a negative effect on the virus replication. Next, data from the Western blot and qRT-PCR analysis showed that HAAS-AV3026

and HAAS-AV3027 attenuated the synthesis of E and NS5 protein, and viral RNA in JEV- and ZIKV-infected cells which endorsed the results of the IFA analysis.

The mechanism of these DHEA derivatives has not been known. Therefore, we investigated the effect of DHEA derivative hit on different steps of the flavivirus life cycle by using a time-addition assay on JEV- and ZIKV-infected Vero cells. The results revealed that HAAS-AV3026 and HAAS-AV3027 worked more efficiently in post-infection treatment, while minimal inhibition on virus titers was also observed even at pre-infection and co-administration treatment. These interesting results enlighten us to elucidate whether these hits intervene in the early steps of the virus life cycle. For this purpose, binding assay, entry assay, and replicon assay were performed, the results of which indicated that DHEA-derived hits did not interfere with the binding and entry of the virus into the cells but inhibited the replication stage of the virus. This means that minimal inhibition in time-addition studies at pre-infection and co-infection treatment might be due to long exposure of compounds to the virus, which ultimately affects the later stage of the virus's life cycle. Collectively, this mechanism study suggests that HAAS-AV3026 and HAAS-AV3027 act primarily at the post-entry process (replication stage) of flaviviruses replication cycle rather than initial steps (entry and binding stage) because no interactions of these hits were observed with host cells receptors.

5. Conclusions

In summary, this study shows the antiviral activity of novel synthetic derivatives of DHEA against flaviviruses (ZIKV and JEV). The observed IC$_{50}$ and cytotoxicity profile together with time-of-addition and molecular mechanism data suggest HAAS-AV3026 and HAAS-AV3027 are potential candidates for treatment.

Data availability

All the data generated during the current study are included in the manuscript.

Ethics statement

This article does not contain any studies with human or animal subjects performed by any of the authors.

Author contributions

Muhammad Imran: methodology, data curation and writing-original draft preparation. Luping Zhang: methodology, data curation and writing-original draft preparation. Bohan Zheng: formal analysis and validation. Zikai Zhao: formal analysis and validation. Dengyuan Zhou: formal analysis and validation. Shengfeng Wan: visualization. Zheng Chen: visualization. Hongyu Duan: formal analysis and validation. Qiuyan Li: data analysis. Xueqin Liu: software validation. Shengbo Cao: conceptualization, supervision and funding acquisition. Shaoyong Ke: methodology, project administration. Jing Ye: conceptualization, project administration and supervision. All authors have read and agreed to the published version of the manuscript.

Conflict of interest

The authors declare that they have no conflict of interest.

Acknowledgments

References

Acosta, E.G., Bruttomesso, A.C., Bisceglia, J.A., Wachsman, M.B., Galagovsky, L.R., Castilla, V., 2008. Dehydroepiandrosterone, epiandrosterone and synthetic derivatives inhibit Junin virus replication in vitro. Virus Res. 135, 203–212.

Ashraf, U., Zhu, B., Ye, J., Wan, S., Nie, Y., Chen, Z., Cui, M., Wang, C., Duan, X., Zhang, H., 2016. Microrna-19b-3p modulates Japanese encephalitis virus-mediated inflammation via targeting Rnf11. J. Virol. 90, 4780–4795.

Bradley, W.G., Kraus, L.A., Good, R.A., Day, N.K., 1995. Dehydroepiandrosterone inhibits replication of feline immunodeficiency virus in chronically infected cells. Vet. Immunol. Immunopath. 46, 159–168.

Chen, Z., Ye, J., Ashraf, U., Li, Y., Wei, S., Wan, S., Zohaib, A., Song, Y., Chen, H., Cao, S., 2016. Microrna-33a-5p modulates Japanese encephalitis virus replication by targeting eukaryotic translation elongation factor 1a1. J. Virol. 90, 3722–3734.

Coleman, D., Leiter, E., Schwizer, R., 1982. Therapeutic effects of dehydroepiandrosterone (DHEA) in diabetic mice. Diabetes 31, 830–833.

Daigle, J., Carr, D.J., 1998. Androstenediol antagonizes herpes simplex virus type 1-induced encephalitis through the augmentation of type I Ifn production. J. Immunol. 160, 3060–3066.

Dalla Valle, L., Couet, J., Labrie, Y., Simard, J., Belvedere, P., Simontacchi, C., Labrie, F., Colombo, L., 1995. Occurrence of cytochrome P450c17 mrna and dehydroepiandrosterone biosynthesis in the rat gastrointestinal tract. Mol. Cell. Endocrinol. 111, 83–92.

Dewald, L.E., Starr, C., Butters, T., Treston, A., Warfield, K.L., 2020. Iminosugars: a host-targeted approach to Combat Flaviviridae infections. Antivir. Res. 184, 104881.

Erlanger, T.E., Weiss, S., Keiser, J., Utzinger, J., Wiedenmayer, K., 2009. Past, present, and future of Japanese encephalitis. Emerg. Infect. Dis. 15, 1.

Fan, W., Qian, S., Qian, P., Li, X., 2016. Antiviral activity of Luteolin against Japanese encephalitis virus. Virus Res. 220, 112–116.

Guo, J., Jia, X., Liu, Y., Wang, S., Cao, J., Zhang, B., Xiao, G., Wang, W., 2020. Screening of natural extracts for inhibitors against Japanese encephalitis virus infection. Antimicrob. Agents Chemother. 64, e02373–19.

Gwon, Y.-D., Strand, M., Lindqvist, R., Nilsson, E., Saleeb, M., Elofsson, M., Överby, A.K., Evander, M., 2020. Antiviral activity of Benzavir-2 against emerging flaviviruses. Viruses 12, 351.

Imran, M., Saleemi, M.K., Chen, Z., Wang, X., Zhou, D., Li, Y., Zhao, Z., Zheng, B., Li, Q., Cao, S., Ye, J., 2019. Decanoyl-arg-val-lys-arg-chloromethylketone: an antiviral compound that acts against flaviviruses through the inhibition of furin-mediated prm Cleavage. Viruses 11, 1011.

Ke, S., Wei, Y., Shi, L., Yang, Q., Yang, Z., 2013. Synthesis of novel steroid derivatives derived from dehydroepiandrosterone as potential anticancer agents. Anti Cancer Agents Med. Chem. 13, 1291–1298.

Labrie, F., Luu-The, V., Labrie, C., BéLanger, A., Simard, J., Lin, S.-X., Pelletier, G., 2003. Endocrine and intracrine sources of androgens in women: inhibition of breast cancer and other roles of androgens and their precursor dehydroepiandrosterone. Endocr. Rev. 24, 152–182.

Laureti, M., Narayanan, D., Rodriguez-Andres, J., Fazakerley, J.K., Kedzierski, L., 2018. Flavivirus receptors: diversity, identity, and cell entry. Front. Immunol. 9, 2180.

Lowe, R., Barcellos, C., Brasil, P., Cruz, O.G., Honório, N.A., Kuper, H., Carvalho, M.S., 2018. The Zika virus epidemic in Brazil: from discovery to future implications. Int. J. Environ. Res. Publ. Health 15, 96.

Mackenzie, J.S., Gubler, D.J., Petersen, L.R., 2004. Emerging flaviviruses: the spread and resurgence of Japanese encephalitis, West Nile and dengue viruses. Nat. Med. 10, S98.

Majewska, M.D., Demirgo, S., Spivak, C.E., London, E.D., 1990. The neurosteroid dehydroepiandrosterone sulfate is an allosteric antagonist of the Gabaa receptor. Brain Res. 526, 143–146.

Mercorelli, B., Palù, G., Loregian, A., 2018. Drug repurposing for viral infectious diseases: How far are we? Trends Microbiol. 26, 865–876.

Misra, U.K., Kalita, J., 2010. Overview: Japanese encephalitis. Prog. Neurobiol. 91, 108–120.

Pedersen, N.C., North, T.W., Rigg, R., Reading, C., Higgins, J., Leutenegger, C., Henderson, G.L., 2003. 16α-Bromo-Epiandrosterone therapy modulates experimental feline immunodeficiency virus viremia: initial enhancement leading to long-term suppression. Vet. Immunol. Immunopathol. 94, 133–148.

Pierson, T.C., Diamond, M.S., 2020. The continued threat of emerging flaviviruses. Nat. Microbiol. 5, 796–812.

Romanutti, C., Bruttomesso, A.C., Castilla, V., Bisceglia, J.A., Galagovsky, L.R., Wachsman, M.B., 2009. In vitro antiviral activity of dehydroepiandrosterone and its synthetic derivatives against vesicular stomatitis virus. Vet. J. 182, 327–335.

Saiz, J.-C., Martín-Acebes, M.A., 2017. The race to find antivirals for Zika virus. Antimicrob. Agents Chemother. 61, e00411–17.

Solomon, T., 2004. Flavivirus encephalitis. N. Engl. J. Med. 351, 370–378.

Wan, S., Ashraf, U., Ye, J., Duan, X., Zohaib, A., Wang, W., Chen, Z., Zhu, B., Li, Y., Chen, H., 2016. Microrna-22 negatively regulates poly (I: C)-Triggered type I interferon and inflammatory cytokine production via targeting mitochondrial antiviral signaling protein (MAVS). Oncotarget 7, 76667.

World Health Organization, 2016. Zika situation report: neurological syndrome and congenital anomalies. https://apps.who.int/iris/handle/10665/204348/. (Accessed 19 December 2020).

Yang, J., Guo, Z., Liu, X., Liu, Q., Wu, M., Yao, X., Liu, Y., Cui, C., Li, H., Song, C., 2020. Cytotoxicity evaluation of chloroquine and hydroxychloroquine in multiple cell lines and tissues by dynamic imaging system and physiologically based pharmacokinetic model. Front. Pharmacol. 11, 574720.

Zhu, B., Ye, J., Nie, Y., Ashraf, U., Zohaib, A., Duan, X., Fu, Z.F., Song, Y., Chen, H., Cao, S., 2015. Microrna-15b modulates Japanese encephalitis virus-mediated inflammation via targeting Rnf125. J. Immunol. 195, 2251–2262.

Zhu, B., Ye, J., Ashraf, U., Li, Y., Chen, H., Song, Y., Cao, S., 2016. Transcriptional regulation of mir-15b by C-Rel and Creb in Japanese encephalitis virus infection. Sci. Rep. 6, 1–15.